Nonlinear Control of Roll Moment Distribution to Influence Vehicle Yaw Characteristics

Daniel E. Williams and Wassim M. Haddad

***Abstract*— The influence of specifying a roll moment distribution to effect the handling dynamics of automobiles has long been appreciated by conventional automotive designers. With the advent of active suspension systems, it is now possible to actively vary the roll moment distribution via feedback control. Nonlinear vehicle dynamics are developed to describe the effect of roll moment distribution. Controllers based on feedback linearization and intuition are developed and simulated. Based on favorable simulation results, the intuitive nonlinear controller was implemented on a passenger automobile and results of its performance are included.**

I. INTRODUCTION

ADVANCED vehicle suspension systems have been widely analyzed in the literature and developed in industry for the past decade. Vehicle suspension systems perform two functions: isolation of the cabin from road noise, and transmission of forces through the tires which accelerate, decelerate, and turn the vehicle. The road noise transmission problem is particularly well posed for the application of linear optimal control theory. Hrovat [1] provides an excellent review of work done in this area. The effect of advanced suspensions on vehicle handling has been largely neglected in the literature, however. Akatsu *et al.* [2] describe handling benefits of a low bandwidth active suspension system using open-loop roll moment distribution. Clover and Bernard [3] report the distribution of lateral load transfer by an advanced suspension can have significant effects on directional stability.

In this paper we make use of the concepts of understeer, neutral steer, and oversteer [4] to develop nonlinear controllers to influence roll moment distribution. For a given turn, side forces generated by the tires establish a moment balance about the center of mass of the vehicle which results in a yaw motion. The centerline of a neutral steering vehicle is tangent to the instantaneous radius of curvature of vehicle trajectory. An oversteering vehicle requires the rear tires to generate relatively large angles of attack in negotiating a turn. The angle the plane of the tire makes with the tire's velocity vector is referred to as the tire's slip angle. To achieve these large slip angles, the rear of the vehicle must present a large angle of attack with respect to the tangent of the radius of curvature of the vehicle path. The opposite of oversteer is understeer. An understeering vehicle needs relatively large slip angles at the front tires, requiring excessive steering input to track a given trajectory. Just as an oversteering vehicle is perceived as twitchy, an understeering vehicle is sluggish.

Although neutral steering characteristics are desired, passenger vehicles generally exhibit varying degrees of understeer. In transient maneuvers, such as heavy acceleration or obstacle avoidance the vehicle can tend toward oversteer. To minimize the occurrence of transient situations where unusual driving skill would be required for control, some degree of understeer is thus designed into the vehicle.

Factors determining the handling characteristic of vehicles include weight bias, tires, suspension kinematics (inducing camber changes) and the related concepts of tire friction circle theory and tire saturation [5]–[10].

Of particular interest in this work is the nonlinear relationship between side force developed by the tire, its slip angle, and the normal force on the tire. As will be shown in Section II, as weight is transferred across an axle in turning, the tire losing normal force loses more side force than the tire which gets the normal force gains in side force. The net result is that weight transfer across an axle reduces its side force, requiring axle tires to generate larger slip angles to achieve a yaw moment balance.

Resistance to body roll can be split between the front and rear axles. In conventional passive suspensions, a relatively high rate stabilizer bar at the front helps support body roll, reducing that axle's net side force and consequently inducing understeer.

Advanced systems such as active suspension [11], [12] and active roll control [13] allow the ability to dynamically distribute the roll moment resistance between front and rear axles. Hence, there is potential to influence the handling dynamics of the vehicle by controlling this roll moment distribution, overcoming static vehicle imbalances and the transient effects introduced above. Such a system would not only improve vehicle performance, but also improve vehicle safety.

II. DYNAMIC VEHICLE MODEL

Many basic vehicle dynamic models have used linear analysis techniques. Consequently, as a first order approximation there is a well defined linear relationship between a tire's slip angle and its generated side force. The resulting change in side force generated by a tire as a function of a change in the normal force on the tire is also well understood. In terms of handling characteristics, however, a linear approximation to this relationship does not improve the vehicle model. Weight

Manuscript received September 1993; revised December 1994. Recommended by Guest Editor, G. Rizzoni.

D. E. Williams is with TRW, Commercial Steering Division, Lafayette, IN 47902 USA.

W. M. Haddad is with the School of Aerospace Engineering, Georgia Institute of Technology, Atlanta, GA 30332 USA.

IEEE Log Number 9408631.

1063–6536/95$04.00

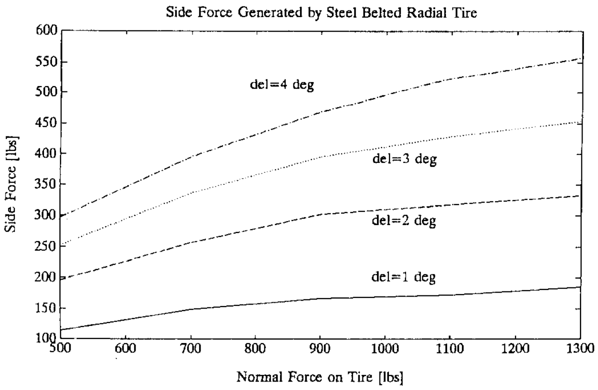

Fig. 1.

is transferred across the vehicle in a turn. One side of the axle gains the normal force that the other side loses. Hence a linear normal force/side force relationship does not improve steady state handling models where the forward speed is assumed constant since the total side force generated by an axle remains constant. As shown in Fig. 1, however, generated side force is a nonlinear function of normal force. Specifically, the data shows that more side force is lost by the subtraction of a certain amount of normal force due to weight transfer in turning on one side of an axle than is gained by the addition of that normal force to the other side.

Intuitively it is preferable to have a tire model which requires both a normal force and a slip angle to generate a side force. Furthermore, to capture the effect of roll moment distribution it is necessary to include the higher order dependence of side force on normal force. With these considerations in mind, an empirical tire model is suggested by [7]

$$Y_i = C_1 \alpha_i N_i + C_2 \alpha_i N_i^2 \tag{1}$$

where Y_i is the side force generated by the ith tire, α_i is the slip angle of the tire, and N_i is the normal force on the tire. C_1 and C_2 are empirical constants to be determined from the data. Assuming the above relationship, a multiple regression analysis [14] was performed on steel belted radial tire data [15]. As expected from the data, the nonlinear tire term C_2 was negative, insuring the desired nonlinear behavior.

In this paper we consider the vehicle model shown in Fig. 2. The vehicle is assumed to be traveling at a constant forward speed, u. Side forces Y are developed at each tire. The model allows two degrees of freedom: yaw, r, and lateral velocity, v. Hence, using small angle approximations, the following differential equations of motion describe the given dynamics

$$m(\dot{v} + ur) = Y_1 + Y_2 + Y_3 + Y_4, \tag{2}$$

$$I_z \dot{r} = a(Y_1 + Y_2) - b(Y_3 + Y_4) \tag{3}$$

where m is the mass of the vehicle, I_z is the yaw moment of inertia, and a and b are distances from the vehicle center of mass to the front and rear axles, respectively.

The side force developed by the front (and rear) tires can be combined to yield the side force generated by the front (and rear) axle. When the left and right tires on an axle are

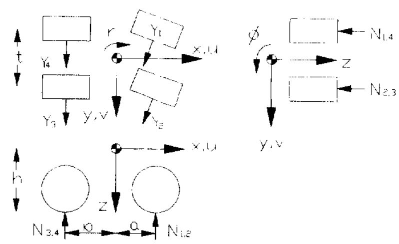

Fig. 2.

combined in this manner, the model is referred to, for obvious reasons, as the bicycle model [10]. In this case

$$\dot{v} = \frac{1}{m}(Y_f + Y_r) - ur \tag{4}$$

$$\dot{r} = \frac{a}{I_z} Y_f - \frac{b}{I_z} Y_r \tag{5}$$

where $Y_f = Y_1 + Y_2$ and $Y_r = Y_3 + Y_4$.

Inserting the previously assumed tire model given by (1), the side forces developed at the front and rear axles can be written as

$$Y_f = \alpha_f (C_1(N_1 + N_2) + C_2(N_1^2 + N_2^2)) \tag{6}$$

$$Y_r = \alpha_r (C_1(N_1 + N_2) + C_2(N_3^2 + N_4^2)) \tag{7}$$

where α_f and α_r are the slip angles experienced by the tires of the front and rear axles, respectively. Using the standard development given in [10] and making use of small angle approximations, the front and rear slip angles can be expressed as

$$\alpha_f = \delta - \frac{ar + v}{u} \tag{8}$$

$$\alpha_r = \frac{br - v}{u} \tag{9}$$

where δ is the steering input.

When a vehicle turns, weight is transferred from the inside wheels to the outside wheels. The magnitude of this weight transfer is a function of mass, speed, yaw rate, and location of the center of mass. This weight transfer must be reacted against by a roll moment produced by the suspension. A conventional suspension would yield front and rear roll stiffness and damping. Differences in these front to rear values would determine the vehicle's roll moment distribution. Given roll stiffness and damping, roll displacement and velocity must be present to yield roll moments. Therefore, adequate treatment of such vehicles would require the inclusion of roll mode dynamics [5]. In this work some form of active roll control system is assumed (specifically an active suspension system [12]) which sufficiently controls roll mode dynamics to justify exclusion. Active roll control also allows a roll moment distribution coefficient to be defined which can range between 1.0 if the roll moment is produced entirely by the front axle and -1.0 if the roll moment is produced entirely at the rear axle. The normal force associated with each tire can be written as

$$N_1 = W\frac{b}{2(a+b)} + mur\frac{h}{t}(1 + \varepsilon) \tag{10}$$

$$N_2 = W\frac{b}{2(a+b)} - mur\frac{h}{t}(1+\varepsilon) \tag{11}$$

$$N_3 = W\frac{a}{2(a+b)} - mur\frac{h}{t}(1-\varepsilon) \tag{12}$$

$$N_4 = W\frac{a}{2(a+b)} + mur\frac{h}{t}(1-\varepsilon) \tag{13}$$

where W is the vehicle weight, h is the height of the center of mass, t is the track, or distance between the centerlines of the tires, and ε is the roll moment distribution defined above. The term mur can be shown to be the steady state inertia force acting on the center of mass, and the term h/t can be thought of as the vehicle aspect ratio. Now, inserting (10)–(13) into (6) and (7) yields

$$Y_f = \alpha_f\Bigg(C_1W\frac{b}{a+b} + \frac{1}{2}C_2W^2\left(\frac{b}{a+b}\right)^2 + 2C_2\left(mu\frac{h}{t}\right)^2(1+\varepsilon)^2r^2\Bigg) \tag{14}$$

$$Y_r = \alpha_r\Bigg(C_1W\frac{a}{a+b} + \frac{1}{2}C_2W^2\left(\frac{a}{a+b}\right)^2 + 2C_2\left(mu\frac{h}{t}\right)^2(1-\varepsilon)^2r^2\Bigg). \tag{15}$$

At this point several observations can be made. When the normal force terms are squared and added together in the axle side force equations (6) and (7), the cross product vanishes, leaving only a term dependent on the static parameters squared and a term proportional to the yaw rate squared and the roll moment distribution. Clearly, the term in the tire model associated with the squared normal force, C_2, is coupled to the roll moment distribution, illustrating the necessity of a nonlinear tire model to study the effect of roll moment distribution on handling. By introducing the notation

$$C_f = C_1W\frac{b}{a+b} + \frac{1}{2}C_2W^2\left(\frac{b}{a+b}\right)^2 \tag{16}$$

$$C_r = C_1W\frac{a}{a+b} + \frac{1}{2}C_2W^2\left(\frac{a}{a+b}\right)^2 \tag{17}$$

$$C_\varepsilon = 2C_2\left(mu\frac{h}{t}\right)^2 \tag{18}$$

(14) and (15) can be re-written as

$$Y_f = \alpha_f(C_f + C_\varepsilon(1+\varepsilon)^2r^2) \tag{19}$$

$$Y_r = \alpha_r(C_r + C_\varepsilon(1-\varepsilon)^2r^2). \tag{20}$$

With this change in notation, C_f and C_r correspond to the familiar tire stiffness coefficients from the linear model. The nonlinear coefficient has been captured in C_ε. As before, the overall sign of the nonlinear term is negative, by virtue of the fact that $C_2 < 0$ and other terms being squared and hence positive.

Using (8) and (9), these results are combined with (4) and (5) to yield the vehicle dynamic model to be used in the

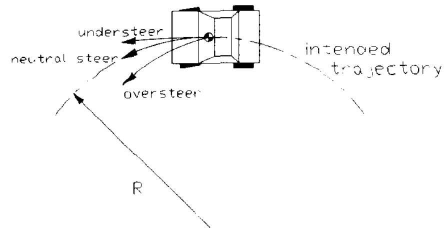

Fig. 3.

remainder of this work. Specifically

$$\dot{v} = -ur + \left(\delta - \frac{ar+v}{u}\right)\left(\frac{C_f}{m} + \frac{C_\varepsilon}{m}(1+\varepsilon)^2r^2\right) + \left(\frac{br-v}{u}\right)\left(\frac{C_r}{m} + \frac{C_\varepsilon}{m}(1-\varepsilon)^2r^2\right) \tag{21}$$

$$\dot{r} = \left(\delta - \frac{ar+v}{u}\right)\left(\frac{aC_r}{I_z} + \frac{aC_\varepsilon}{I_z}(1+\varepsilon)^2r^2\right) - \left(\frac{br-v}{u}\right)\left(\frac{bC_r}{I_z} + \frac{bC_\varepsilon}{I_z}(1+\varepsilon)^2r^2\right) \tag{22}$$

which can be referred to as the nonlinear bicycle model. The two first order differential equations are coupled. Both equations are quadratic in the control variable ε, and cubic in the yaw rate r.

III. Handling Characteristics

In this section we formalize the previous qualitative discussion of vehicle handling. The steering angle input necessary for a vehicle to negotiate a steady state turn can be expressed as [10]

$$\delta = \frac{a+b}{R} + K_{us}\frac{u^2}{gR} \tag{23}$$

where K_{us} is referred to as the understeer gradient and is expressed in radians, g is the gravitational constant, and R is the radius of curvature. If $K_{us} = 0$, the steering input is a function of vehicle wheelbase and the radius of curvature of the desired trajectory. Notably, given this neutral steer condition, the steer angle is independent of vehicle speed. If $K_{us} > 0$, increasing steering input will be necessary to negotiate the desired trajectory as forward speed u increases. As mentioned earlier, this is called understeer. Alternatively, if $K_{us} < 0$, as speed increases for a given maneuver, steering input decreases which corresponds to an oversteering condition. The desirability of a neutral steering vehicle is apparent. These three handling characteristics are illustrated in Fig. 3.

Next, (23) can be manipulated to a more convenient form for vehicle characterization and control purposes. Specifically, by noting that the steady state radius of curvature can be expressed as the forward speed divided by the yaw rate, (23) can be re-written as

$$\delta = \frac{r(a+b)}{u} + K_{us}\frac{ur}{g} \tag{24}$$

which can directly be used for vehicle measurement and control as the required variables are easily measured. Forward speed u is readily available on most vehicles as a pulse train, angular rate sensors are commercially available (Systron Donner, Concord CA), and linear position sensors which can be installed on the steering rack are available from a variety of sources.

Equation (25) can be used to illustrate the feedback nature of the control problem. Specifically

$$e = \delta\left(\frac{ug}{g(a+b) + K_{us}u^2}\right) - r. \tag{25}$$

The steering input δ is modified to become a desired yaw rate, given the desired understeer coefficient K_{us}, vehicle speed u, and wheelbase $(a+b)$. The measured yaw rate r is subtracted from the desired yaw rate to yield a yaw rate error e. The control task can be seen to be a trajectory tracking problem. The driver commands a desired yaw rate trajectory; a control system is desired which influences the vehicle dynamics so that the yaw rate error is minimized.

IV. Nonlinear Controller Design

A control law for the given system will be developed using the input-output linearization method outlined by Slotine and Li [16]. Specifically, given the nonlinear system

$$\dot{x} = f(x, \varepsilon) \tag{26}$$

$$y = h(x) \tag{27}$$

where $x \in \mathcal{R}^n$ is the state vector, $\varepsilon \in \mathcal{R}^m$ is the control input, $y \in \mathcal{R}^l$ is the system output, $f : \mathcal{R}^n \times \mathcal{R}^m \to \mathcal{R}^n$, and $h : \mathcal{R}^n \to \mathcal{R}^l$. Slotine and Li summarize the feedback linearization process in three steps:

1) differentiate the output y until the input ε appears;
2) choose ε to cancel the nonlinearities and guarantee tracking convergence; and
3) study the stability of the internal (unobserved) dynamics.

As we formulate this specific tracking problem, the output is the tracking error, previously defined by (25), assuming $K_{us} = 0$ for neutral steering. Differentiating (25) with respect to time yields

$$\frac{d}{dt}e = \dot{\delta}\left(\frac{u}{a+b}\right) - \dot{r}. \tag{28}$$

Using (22) the control variable ε now explicitly appears in (28). Hence, if a control variable can be found which satisfies

$$\dot{e} + Ke = 0 \tag{29}$$

tracking convergence is guaranteed via convergence of linear error dynamics, where K is a positive constant. Inserting (28) and (22) into (29) yields

$$\begin{aligned}
&\varepsilon^2 \frac{C_\varepsilon}{I_z u}(\delta r^2 au - r^3(a^2+b^2) + r^2 v(b-a)) \\
&+ \varepsilon \frac{2C_\varepsilon}{I_z u} r^2(\delta au - r(a^2-b^2) - v(b+a)) \\
&+ \frac{C_\varepsilon}{I_z u} r^2(\delta au - r(a^2+b^2) + v(b-a)) \\
&- \frac{1}{I_z u}(\delta au C_f - r(a^2 C_f + b^2 C_r) + v(bC_r - aC_f)) \\
&- \dot{\delta}\frac{u}{a+b} + K\left(r - \delta\left(\frac{u}{a+b}\right)\right) = 0.
\end{aligned} \tag{30}$$

The exact solution of the above equation insures that the tracking error converges to zero. Of course ε must be between -1 and 1. If no real solution exists, or if a real solution is out of the -1, 1 interval, ε is set to 1 if the vehicle is oversteering or -1 if understeering. As the value of K is increased, ε saturates more. At the extreme, if K is very large, ε is either 1 or -1 dependent upon the understeer/oversteer condition of the vehicle. This controller thus resembles a variable structure controller, of which sliding mode control is the most notable. It can be shown that while the system formed by (21), (22), and (25) does not fit into the class of problems to which the sliding mode control method strictly applies, a variable structure controller can be synthesized in a method similar to the sliding mode development which results in (30) with the above saturation constraints [17]. As common with variable structure controllers of this type, large values of K result in very good disturbance rejection properties, however, the control begins to resemble pulse width modulation, which can excite unmodeled modes, particularly structural modes.

Internal dynamics are not directly considered in the formulation of the control strategy. The internal dynamics of a nonlinear system are similar to the unobservable dynamics of a linear system in that they have no effect on the input-output dynamics established by (25). In the present formulation the internal dynamics of the system are given by the lateral velocity described in (21).

If perfect tracking is assumed, the yaw rate can be expressed in terms of the steering input

$$r = \left(\frac{u}{a+b}\right)\delta. \tag{31}$$

Now, substituting (31) into (21) the internal dynamics are described by

$$\begin{aligned}
\dot{v} = &-\frac{u^2}{a+b}\delta + \delta^2\frac{b}{a+b} \\
&\cdot\left(C_f + C_r + 2C_\varepsilon\left(\frac{u\delta}{a+b}\right)^2(1+\varepsilon^2)\right) \\
&- \frac{v}{mu}\left(C_f + C_r + 2C_\varepsilon\left(\frac{u\delta}{a+b}\right)(1+\varepsilon^2)\right).
\end{aligned} \tag{32}$$

Nothing can be determined about the stability of (32) for a nonzero δ. However, if δ is zero, (32) is stable using reasonable values of C_ε. Slotine and Li [16] refer to this condition as the zero dynamics and point out that global stability of the internal dynamics is not assured by stable zero dynamics. Only local stability of the internal dynamics is guaranteed.

An alternative to the above formulation is the intuitive nonlinear yaw strategy given by

$$\varepsilon = K_{yaw}\left(|r| - \frac{u}{a+b}|\delta|\right) \tag{33}$$

where K_{yaw} is a strictly positive constant. Quite simply, if the vehicle's yaw rate is greater than desired (oversteer), the roll moment is carried more by the front axle, alternatively, if the vehicle is understeering, the roll moment is carried more on the rear axle. (For completeness, a check for countersteering should be made. If r and δ have different signs, then $\varepsilon = 1$.

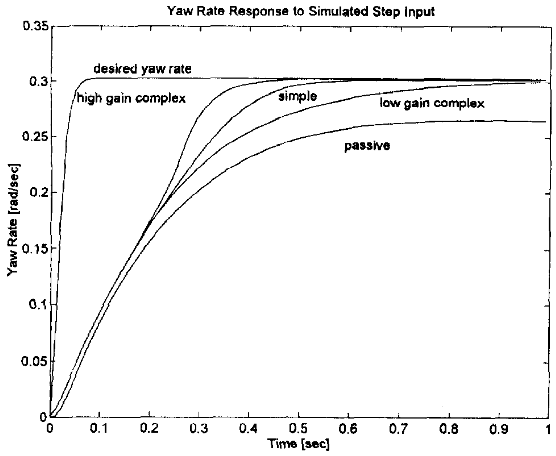

Fig. 4.

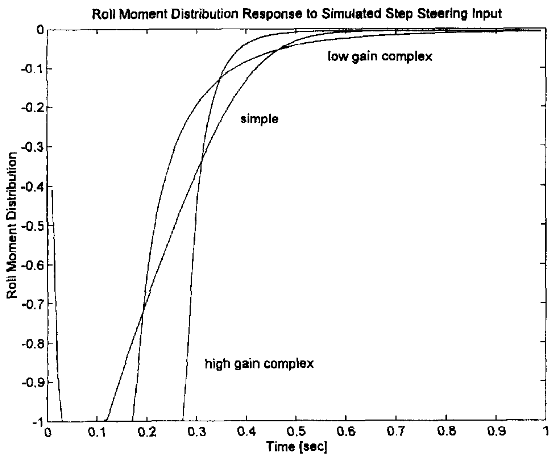

Fig. 5.

When implemented this extreme oversteer situation did not occur in the limited testing described in Section VI.)

V. Simulation Results

A nonlinear control law satisfying (30) was simulated using two different values for K. The yaw response to a large rate limited step steering input is shown in Fig. 4 with the roll moment distribution shown in Fig. 5. Results based on satisfying (30) are referred to in both figures as high and low gain complex control. Also shown is the result using the simple intuitive controller given by (33), as well as a similar passively suspended vehicle with a 60/40 roll stiffness distribution front to rear.

Upon the initial steering input, a large yaw error is built up even with the roll moment distribution saturated at the rear. Several effects contribute to this lag, the first is the response time of the linear yaw dynamics of the vehicle is slower than the steering input. Second, for the closed yaw rate loop to have significant control authority, weight transfer must be present so that it can be distributed. Consequently, the control system must work very hard to initiate a yaw rate, but has more authority as the yaw rate response increases. As shown in (22), the roll moment distribution term ε is multiplied by the yaw rate r raised to the third power.

Both complex nonlinear control strategies exhibit zero steady state tracking errors with the lower gain complex controller converging more slowly. Comparing the low gain complex controller and the controller employing the simple intuitive yaw strategy with an equivalent yaw error gain ($K_{\text{yaw}} = K$), it can be seen that the simple yaw strategy exhibits a nonzero steady state error, but converges more quickly. The simulation work revealed that the closed-loop system is stable for large values of tracking error gains, using either the simple intuitive controller suggested in (33) or the full nonlinear controller satisfying (30). Response time of the complex and simple controllers are similar. In fact, the fundamental limitation of the system response time was not the particular control strategy, rather the fact that all controllers initially saturate the roll moment distribution at the rear. Although the complex controller insures zero steady state tracking error, deviations from neutral steer using the simple intuitive controller can be made small by increasing the stiffness K_{yaw}.

VI. Experimental Vehicle Results

The intuitive yaw rate controller strategy given by (33) was implemented in a full sized passenger sedan. The vehicle was fitted with a broad bandwidth active suspension similar to that described by Goran *et al.* [12]. The simple strategy was selected over the more complex feedback linearization controller strategy due to its computational simplicity, number of required sensors, and knowledge of vehicle parameters, coupled with the simulation results. The simple strategy of (33) requires three vehicle measurements, yaw rate, steering rack displacement, and vehicle speed. Vehicle speed is currently available, yaw rate and steering rack displacement are likely to be measured on vehicles as future generation Anti-Lock Brake systems (ABS) and steering control systems such as steer by wire and rear wheel steer appear.

The complex controller requires knowledge of vehicle inertial properties, tire properties, center of gravity location, and steering input rate, as well as the inputs required by the simple controller. The inertia properties and center of gravity location vary with time. Tire properties required by the controller are the result of the tire model used. The tire model was selected as the simplest model which captured the fundamental nonlinear behavior of interest. Actual tire behavior will deviate from the model. When the complex model based controller is confronted with these parametric variations, it is likely that its performance will be no better and perhaps worse than the simple intuitive strategy since robustness issues are not explicitly accounted for by the feedback linearization controller.

We propose that the real value in the feedback linearization development is much the same as that of LQG based controllers in industry. While a few LQG controllers are no doubt actually implemented, the vast majority of industrial controllers are of classical design. LQG theory, however, is quite useful in providing a benchmark by which actual controllers are measured. Similarly, we have used the feedback

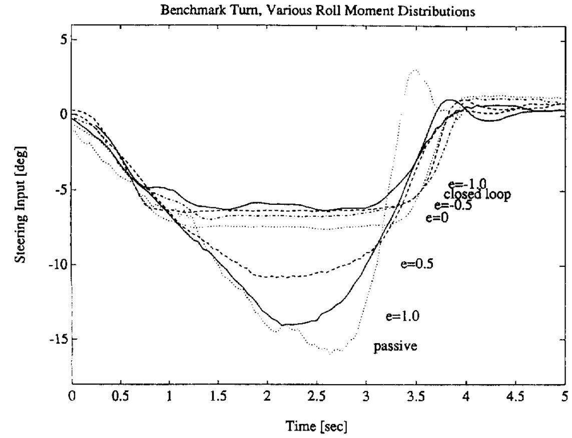

Fig. 6.

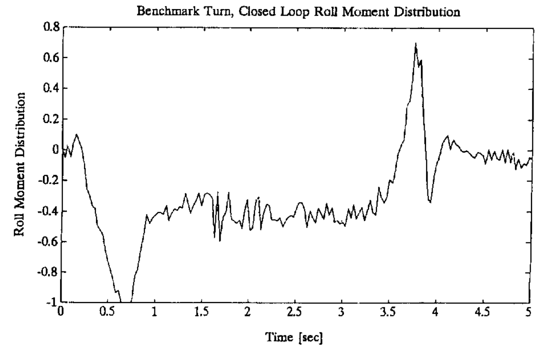

Fig. 7.

linearization approach to validate the performance of the simple intuitive controller.

Fig. 6 shows the steering input required to maneuver the vehicle through a relatively sharp single lane 90 degree turn at 30 mph for various static roll moment distribution parameters, as well as the closed-loop case. With the forward speed controlled and the radius of curvature constrained, the yaw rate response was largely defined. Variation between different vehicle conditions was most apparent in the steering input required for the vehicle to track the well defined trajectory.

For large negative roll moment distributions the vehicle requires constant steering corrective effort. For positive roll moment distributions, the vehicle requires large progressive steering inputs. For both the closed-loop case and the equal roll moment distribution condition, the steering input is desirable. The input quickly reaches the required value and the driver is able to maintain the desired trajectory for the duration of the maneuver with little additional control input.

The closed-loop vehicle has a peculiar, but not necessarily offensive feel to it. As shown in Fig. 7, when the maneuver is initiated, the roll moment is carried on the rear, "loosening" the rear wheels. A driver not experienced with the closed-loop vehicle may find this effect disconcerting. Although the vehicle technically does not oversteer based on (24), it seems that perhaps initially the driver is sensitive to higher than anticipated yaw accelerations. As the driver develops confidence in the control system's ability to "loosen" the car to quickly develop yaw rates and let the rear wheels "bite" when the desired yaw rate has been established, the driving sensation can be pleasant.

For drivers not comfortable with the sensation of trusting the control system to "loosen" the vehicle, several modifications were made in the yaw strategy. First, the minimum roll moment distribution was limited to -0.5. Second, the steering input was low-pass filtered to decrease the control system's response to sudden steering inputs. For typical passenger vehicles this controller still allows moderate roll moments to be carried on the rear axle, while not demanding excessive rearward roll moment distribution due to a steering wheel input that cannot be tracked due to the limitations in the yaw dynamics of the vehicle.

Also shown in Fig. 6 is the steering input required for the same vehicle with a passive suspension. The closed-loop active vehicle requires a constant lower steering input to track the trajectory whereas the passive vehicle requires a progressively increasing steering input. During this maneuver the front tires of the passive vehicle were nearly saturated; which in fact determined the forward velocity of the test. It is instructive to compare the passive vehicle with the active vehicle with the roll moment carried entirely on the front axle ($\epsilon = 1.0$). The passive vehicle uses a front stabilizer bar, but the roll moment remains partially distributed between the front and rear load springs. The improvement in handling between these two vehicles is due to the active suspension eliminating body roll which reduces the effects of sprung mass dynamics and camber changes on vehicle handling.

An advantage of the closed-loop yaw control system not to be overlooked is the safety aspect. For performance, the roll moment distribution is allowed to move rearward if necessary. Just as important is the fact that the roll moment distribution can move forward if for some reason the rear becomes too "loose." This effect can be seen in Fig. 7 where at the exit of the turn the roll moment is carried by the front axle. Although not demonstrated in this work, more extensive vehicle testing is likely to show that a closed-loop yaw rate control system not only improves vehicle performance, but increases driver confidence in an emergency maneuver.

REFERENCES

[1] D. Hrovat, "Applications of optimal control to advanced automotive suspension design," *ASME J. of Dynamic Systems, Measurement, and Control*, June 1993.
[2] Y. Akatsu, N. Fukushima, K. Takahashi, M. Satoh, and Y. Kawarazaki, "An active suspension employing an electrohydraulic pressure control system," SAE paper 905123, 1990.
[3] C. L. Clover and J. E. Bernard, "The influence of lateral load transfer distribution on directional response," SAE paper 930763, 1993.
[4] Society of Automotive Engineers, "Vehicle dynamics terminology," SAE paper j670e, 1970.
[5] J. R. Ellis, *Vehicle Dynamics*. London, England: Business Books, 1979.
[6] J. R. Ellis, *Road Vehicle Dynamics*. Akron, OH: Ellis, 1989.
[7] T. D. Gillespie, *Fundamentals of Vehicle Dynamics*, SAE, 1992.
[8] C. Campbell, *Automobile Suspensions*. London: Chapman and Hall, 1981.
[9] D. Bastow and G. Howard, *Car Suspension and Handling*. London: Pentech Press, 1993.
[10] J. Y. Wong, *Theory of Ground Vehicles*. New York: Wiley, 1978.
[11] W. F. Milliken, Jr., "Active suspension," SAE paper 88079.

[12] M. Goran, B. Bachrach, and R. Smith, "The design and development of a broad bandwidth active suspension concept car," *FISITA*, 1992.
[13] A. Whydell, I. Crawford, R. Williams, S. Miller, and D. Mulvein, "Active roll control," in *Proc. Ford 6th Worldwide Vehicle Dynamics Conf.*, 1992.
[14] G. E. P. Box, W. G. Hunter, and J. S. Hunter, *Statistics for Experimenters.* New York: Wiley, 1978.
[15] L. D. Metz, *Vehicle Dynamics Seminar Notes.*
[16] J. J. Slotine and W. Li, *Applied Nonlinear Control.* Englewood Cliffs, NJ: Prentice-Hall, 1991.
[17] D. E. Williams, Ph.D. dissertation to appear, Florida Institute of Technology, Melbourne, FL.

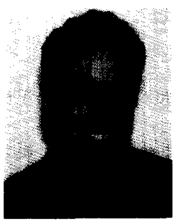

Daniel E. Williams received the B.S. and M.S. degrees from the University of Illinois, Urbana, IL, in 1985 and 1987. In 1990 he received the M.B.A. degree from the Florida Institute of Technology, Melbourne, FL. He is currently a Ph.D. candidate in the Mechanical Engineering Department at the Florida Institute of Technology.

From 1987 to 1994 he worked as Project, Systems, and then Senior Systems Engineer for the Active Control Systems Division of TRW. In 1994 he was named Chief Engineer for Advanced Systems of TRW Commercial Steering Division. His professional interests are in the areas of vehicle control systems and vehicle dynamics. He has received three patents for his work in advanced suspensions, with two other applications pending.

He is a member of Tau Beta Pi and a Registered Professional Engineer.

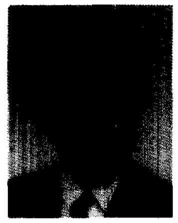

Wassim M. Haddad received the B.S., M.S., and Ph.D. degrees in mechanical engineering from the Florida Institute of Technology, Melbourne, FL, in 1983, 1984, and 1987, respectively, with specialization in dynamics and control.

Since 1987 he has been a consultant for the Structural Controls Group of the Government Aerospace Systems Division, Harris Corporation, Melbourne, FL. In 1988 he joined the faculty of the Mechanical and Aerospace Engineering Department at Florida Institute of Technology where he founded and developed the Systems and Control Option within the graduate program. Since 1994 he has been a member of the faculty in the School of Aerospace Engineering at the Georgia Institute of Technology, Atlanta, GA, where he holds the rank of Associate Professor. His current research interests are in the areas of linear and nonlinear robust multivariable control for aerospace systems, absolute stability theory, fixed-architecture control, mixed-H_2/μ analysis and synthesis for systems with nonlinear structured uncertainty, and saturation control, particularly as applied to vibration control of large flexible structures. He has concentrated on the development of an integrated control-system design methodology for robust, high-performance controllers satisfying multiple design criteria (H_2/H_∞) and real-world hardware constraints within continuous-time, discrete-time, and sampled-data settings.

Dr. Haddad is a recipient of the National Science Foundation Presidential Faculty Fellow Award and is a member of Tau Beta Pi.